Dynamics of an oscillating bubble in a narrow gap

Citation: Azam, Fahad Ibn, Badarinath Karri, Siew-Wan Ohl, Evert Klaseboer, and Boo Cheong Khoo. "Dynamics of an oscillating bubble in a narrow gap." Physical Review E 88, no. 4 (October 2013). © 2013 American Physical Society

As Published: http://dx.doi.org/10.1103/PhysRevE.88.043006

Publisher: American Physical Society

Persistent URL: http://hdl.handle.net/1721.1/84922

Version: Final published version: final published article, as it appeared in a journal, conference proceedings, or other formally published context

Dynamics of an oscillating bubble in a narrow gap

Fahad Ibn Azam
Department of Mechanical Engineering, National University of Singapore, Kent Ridge, Singapore 119260

Badarinath Karri
Singapore-MIT Alliance, 4 Engineering Drive 3, Singapore 117576

Siew-Wan Ohl and Evert Klaseboer
Institute of High Performance Computing, 1 Fusionopolis Way, #16-16 Connexis, Singapore 138632

Boo Cheong Khoo*
Department of Mechanical Engineering, National University of Singapore, Kent Ridge, Singapore 119260 and Singapore-MIT Alliance, 4 Engineering Drive 3, Singapore 117576

(Received 2 May 2013; revised manuscript received 12 August 2013; published 14 October 2013)

The complex dynamics of a single bubble of a few millimeters in size oscillating inside a narrow fluid-filled gap between two parallel plates is studied using high-speed videography. Two synchronized high-speed cameras were used to observe both the side and front views of the bubble. The front-view images show bubble expansion and collapse with the formation of concentric dark and bright rings. The simultaneous recordings reveal the mechanism behind these rings. The side-view images reveal two different types of collapse behavior of the bubble including a previously unreported collapse phenomenon that is observed as the gap width is changed. At narrow widths, the bubble collapses towards the center of the gap; when the width is increased, the bubble splits before collapsing towards the walls. The bubble dynamics is also observed to be unaffected by the hydrophobic or hydrophilic nature of the plate surface due to the presence of a thin film of liquid between each of the plates and the bubble throughout the bubble lifetime. It is revealed that such systems do not behave as quasi-two-dimensional systems; three-dimensional effects are important.

DOI: 10.1103/PhysRevE.88.043006 PACS number(s): 47.55.dp, 47.55.dd, 47.55.df

I. INTRODUCTION

The dynamics of a single cavitation bubble in an unbounded liquid (the so-called free-field bubble) as well as a bubble in a semiunbounded system such as a bubble near a free-surface or a rigid boundary have been extensively studied in the literature. In many real situations, however, cavitation bubbles occur within confined spaces and narrow gaps. Some examples include bubbles used to actuate flows within microfluidic devices [1,2], bubbles used for cell lysis and drug delivery [3,4], as flow controllers [5], and bubbles used for ultrasonic cleaning [6]. We report here on the dynamics of a bubble within a narrow gap between two closely spaced parallel plates.

There are few previous studies in the literature on the dynamic behavior of bubbles within narrow gaps. Kucherenko and Shamko [7] first presented experimental observations of a bubble between two glass plates using a camera. The bubbles were in most cases recorded from the side which shows the evolution of the bubble shape and profile. In a few cases the bubble was also recorded from the front [the reader is referred to Fig. 1(a) for what we mean by side and front views]. However, the recordings of the front and the side views were not simultaneously performed but obtained from separate experiments. They reported on the behavior of bubbles that are symmetrical (i.e., with the bubble center exactly at the center of the gap) and also asymmetrically created bubbles (i.e., with the bubble center closer to one plate than the other). Ishida *et al.* [8] reported numerical and experimental work on the dynamics of a bubble oscillating in a gap between two parallel plates. They demonstrated that the shape of the bubble is dependent upon the nondimensional gap width W', which is defined as the ratio of the gap width between the plates W to the maximum bubble radius R_m, i.e., $W' = W/R_m$. The study however focused only on $W' \sim 2$. In both studies above, the photographs reveal the difference in collapse behavior (as seen in the side-view images) between the cases when the bubble is symmetrical and when it is asymmetrical. In case of a symmetrical bubble, the bubble splits at its center as it collapses after expansion. Each of the split parts of the bubble then moves towards the nearest plate and collapses. When the bubble is asymmetrically created, the bubble assumes a conical shape and collapses towards one plate.

At a smaller length scale, Quinto-Su *et al.* [9] studied laser-generated bubbles of a few micrometers in size within microfluidic gaps of a few micrometers using a high-speed camera. Here, the bubbles were recorded only from the front and the study focused on the bubble behavior over a range of gap widths beginning with $W' = 0.26$ to W' going to ∞, i.e., with the upper plate removed. Gonzalez-Avila *et al.* [10] have also studied the jetting behavior of laser-generated bubbles within narrow gaps as the gap width is changed with W' starting from 0.4. They recorded the phenomena in the side view. By virtue of the design of the setup, the bubbles generated in both studies were asymmetrical.

In this paper, we focus on the dynamics of a symmetric oscillating bubble within a narrow gap formed by two parallel

*mpekbc@nus.edu.sg

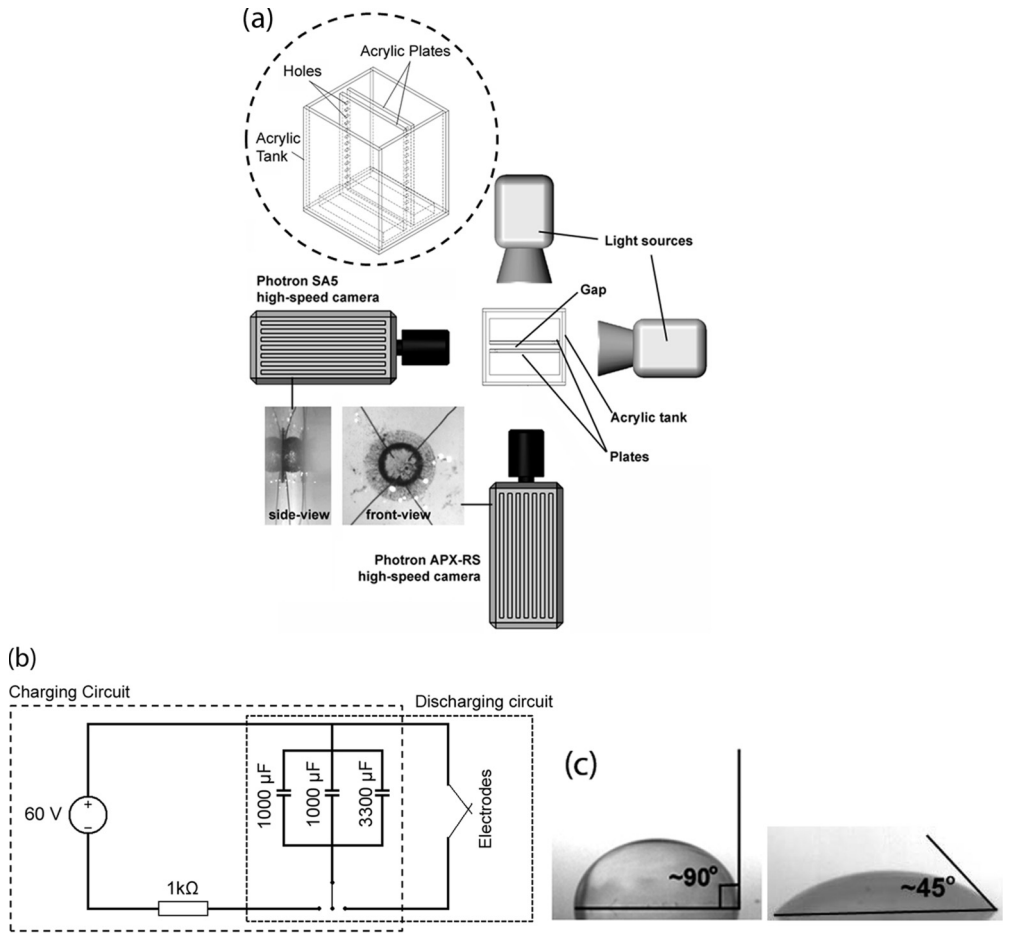

FIG. 1. (a) Schematic of the experimental setup used for the study of bubbles oscillating in a narrow gap. (b) The electric circuit used to create the bubble. (c) The contact angle of a water drop on a silanized glass plate (hydrophobic) and on a hydrophilic acrylic plate.

plates for bubbles in the millimeter size range and over a range of gap widths W' ranging from 0.3 to 3.0. We used two synchronized high-speed cameras, which recorded the bubble from both the front and the side simultaneously. The front-view images show the presence of concentric dark and bright rings whose size and position change as the bubble oscillates. Although such rings have been observed in the images from earlier studies (see Fig. 2(a) in Kucherenko and Shamko [7], Figs. 2(a)–2(c) in Quinto-Su *et al*. [9]), there is minimal discourse on their physical interpretation and their formation is not well understood. Our recordings reveal the sequence of events leading to the rings. The bubble dynamics is found to be dependent on the gap width W' between the plates. A previously unreported bubble collapse behavior is discussed here wherein at low W', the bubble surface that is not on the plates oscillates between a convex and a concave surface curvature a couple of times. The bubble eventually collapses towards the center of the gap. This is different from the collapse at higher W', when the bubble splits at its center with each of the split parts collapsing towards the closest wall. This latter collapse behavior is similar to that reported in the literature [7,8] but the behavior at low W' has not been reported in the literature to the authors' best knowledge. We also studied the effect of the surface wettability of the plate (hydrophilic or hydrophobic nature) on the bubble dynamics. We show that the bubble behavior remains unchanged for both types of plates under similar conditions of gap width and bubble size. This is most likely due to a thin film of liquid, which is always present between the bubble and each of the plates and does not drain out as the bubble expands. The observations indicate that the presence of the thin film negates the effect of the surface characteristics.

II. EXPERIMENTAL SETUP AND PROCEDURE

The experimental setup used in the study is shown in Fig. 1(a). It is comprised of a transparent acrylic tank to hold the liquid, two acrylic plates with a supporting base and holes on their sides, an electrical circuit to create the bubble, and two cameras and illumination setup to record the phenomenon. The tank had dimensions of $120 \times 110 \times 150$ mm^3 and is filled with water up to 90% of its volume. The two acrylic plates were placed parallel to each other inside the tank to form the narrow gap. The plates had dimensions of 100×80 mm^2 and a thickness of 10 mm each. The electrode wires used to create the spark bubble were passed through the holes (diameter 2 mm) on the sides of each of the two plates and made to cross each other in the center of the gap between the plates. In order to vary the gap width, small pieces of acrylic of dimensions 10×10 mm^2, and with thickness of 1.5, 2, or 2.5 mm were

used as spacers. The spacer pieces were placed one on top of another between the plates to get the required gap width W. The plates were then clamped together to keep the gap width fixed during the course of the experiment.

The bubble is created using a low-voltage electrical spark circuit with capacitors as described in earlier studies [11,12] and also shown schematically in Fig. 1(b). The capacitors were first charged to about 59 V using the resistor in the circuit and then short circuited through the electrodes (0.1 mm diameter copper wires) using a two-way switch. Upon short circuiting, a bubble is created at the crossing point of the contacting electrodes, expands and collapses against the plates. The bubble dynamics were recorded both from the front as well as the side of the plates simultaneously using two synchronized high-speed cameras as shown in Fig. 1(a). Some sample images of the front and side view are also shown. Both cameras were operated at 30 000 frames per second with an exposure time of 12 μs.

III. RESULTS AND DISCUSSION

A. Effect of gap width

Figure 2 shows a sequence of eight images to describe the evolution of the bubble between the plates. The numbers at the top indicate the time (in ms). Each image in the sequence consists of two frames—the left frame shows the observation recorded from the front, and the right frame shows the observation recorded from the side. The maximum bubble radius R_m = 4.3 mm was measured vertically in the central plane between the parallel plates using the side-view images. The gap width W between the plates is W = 3.7 mm, and the dimensionless gap width $W' = W/R_m = 0.86$ for this case [13].

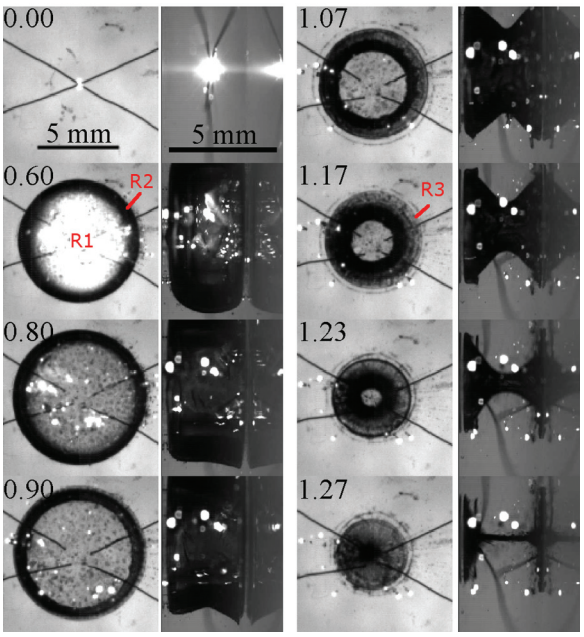

FIG. 2. (Color online) Bubble oscillating at the center of a narrow fluid filled gap of width W = 3.7 mm between two acrylic plates. The bubble reaches its maximum radius of R_m = 4.3 mm. The nondimensional gap width is $W' = 0.86$. There are eight images in the sequence arranged top to bottom in two columns. Each image consists of two frames one from each of the two cameras recording the front view (left frame) and side view (right frame) of the phenomenon simultaneously. The numbers at the top indicate the time in ms. Note the change in curvature of the bubble in the side view from an outward convex surface to an inward concave surface as the bubble expands and then collapses.

The bubble is created at $t = 0.00$ ms, and expands to its maximum radius by $t = 0.60$ ms with a convex surface curvature as noted in the side view (see bottom of bubble). In the front-view image, we observe a bright central region due to the still existent spark which we now refer to as region R1 as shown in Fig. 2. The bright center is surrounded by a dark ring denoted as region R2. By $t = 0.80$ ms, the bubble surface begins to curve inwards as it shrinks and is almost flat (side view). The region R1 is also now grayish in color due to the spark having died down. At $t = 1.07$ ms, a third distinct region R3 (lighter gray) is observed, which surrounds the regions R1 and R2. The side-view image at $t = 1.17$ ms gives us an idea of what each of the regions R1, R2, and R3 in the front view are due to. Region R1 is lighter (gray) due to the light passing through the entire bubble in the central portion of the bubble. Region R2 (dark) is due to the fold of the bubble wall as a result of which the light has to pass through both the bubble and the liquid in its path. Region R3 corresponds to the portion of the bubble sticking to the wall, i.e., the boundary layer, even as the rest of the bubble shrinks. The boundary layer can be seen as a dark line on the plate walls in the side view particularly at $t = 1.27$ ms. In the period from $t = 1.17$–1.27 ms, the bubble surface curvature also becomes more concave and it begins to split in the center with each portion collapsing towards the nearest wall (side view). This corresponds to the shrinking size of the regions R1 and R2 in the front views. Finally by $t = 1.27$ ms, the bubble has split with each part collapsing fully and then the two split portions are connected by a thin line of bubble remnants. The bubble collapse behavior observed here is similar to that shown by Ishida *et al.* [8] (their Fig. 2) and Kucherenko and Shamko [7] [their Fig. 2(b)]. However, the simultaneous side and front views shown here give an insight into the dark and light regions that are observed and the effect of the boundary layer where the portion of the bubble near the wall remains attached to the wall even as the rest of the bubble collapses.

We now present two cases that show a different bubble collapse behavior. Figures 3 and 4 show a bubble at reduced nondimensional gap widths of $W' = 0.56$ and 0.38 respectively [13]. In Fig. 3, the bubble is created at $t = 0.00$ ms and expands with a convex curvature (as seen in the side view at $t = 0.37$ ms) and at $t = 0.67$ ms reaches its maximum radius with an observed flat surface. A grayish region R1 surrounded by a dark region R2 is also noted in the front view similar to the case in Fig. 2. Region R3 due to the boundary layer is first seen at $t = 0.93$ ms (front view) and remains till the end of the bubble collapse. At this time ($t = 0.93$ ms) the bubble surface is concave (side view). The bubble behavior until this time shows a correspondence with the case in Fig. 2. However, from $t = 0.93$–1.23 ms, a different bubble behavior is observed. The bubble surface flattens first ($t = 1.13$ ms) and becomes convex again ($t = 1.23$ ms) as seen in the side view even as the bubble shrinks in size. The bubble then continues

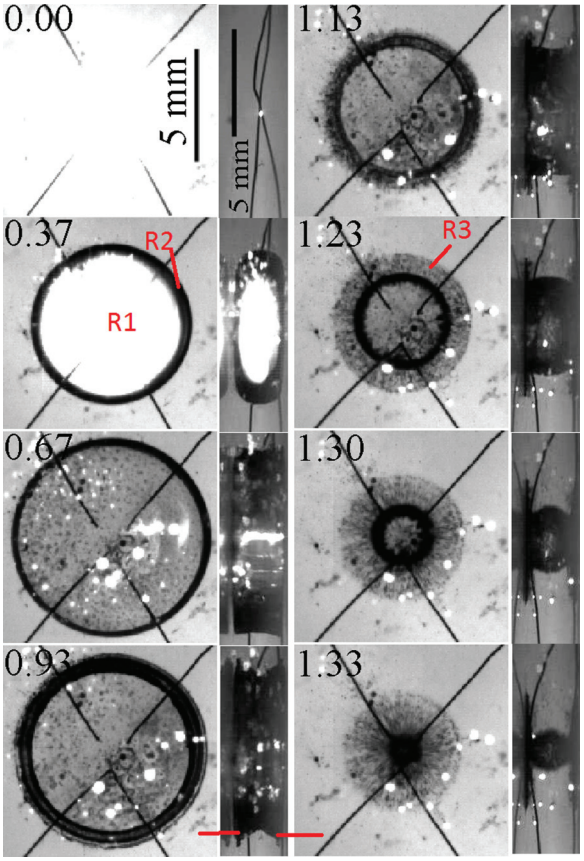

FIG. 3. (Color online) A bubble oscillating in a narrow gap at a nondimensional gap width and maximum bubble radius of $W' = 0.56$ and $R_m = 4.2$ mm respectively. A set of eight images is shown arranged top to bottom in two columns. Each image is comprised of two frames, one from each of the two cameras recording the front view (left frame) and the side view (right frame). The numbers at the top indicate time in ms. Note that the bubble in this case collapses towards the center of the gap between the plates unlike the case in Fig. 2.

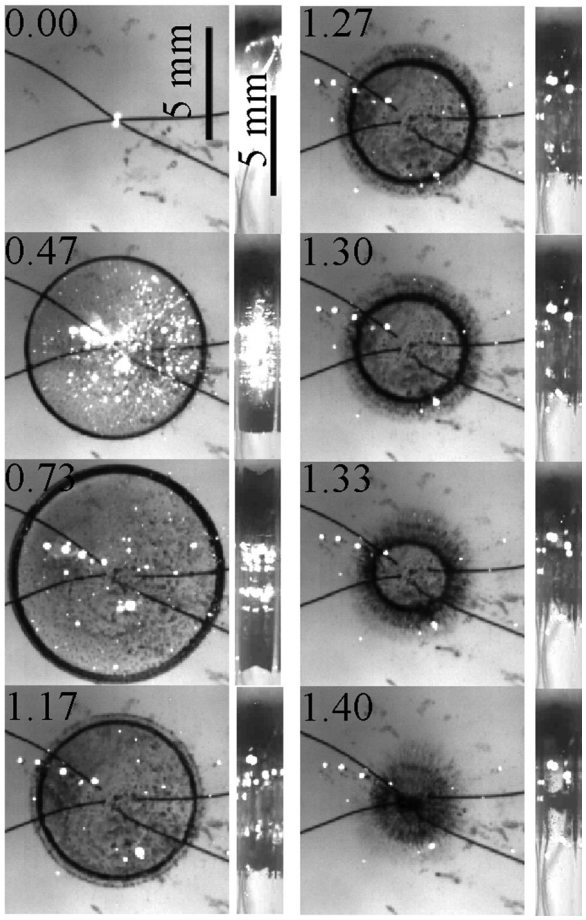

FIG. 4. A bubble oscillating in a narrow gap at a low nondimensional gap width and maximum bubble radius of $W' = 0.38$ and $R_m = 4.8$ mm respectively. A sequence of eight images is shown arranged top to bottom in two columns. Each image comprises of two frames, one from each of the two cameras recording the front view (left frame) and the side view (right frame). The numbers at the top indicate time in ms. Note the two cycles of change in the bubble surface curvature from convex to concave to convex again between $t = 0.47$–1.40 ms when the bubble collapses.

to shrink with a convex curvature ($t = 1.30$ ms) and collapses towards the center at $t = 1.33$ ms. This is unlike the case in Fig. 2 where the bubble split and collapsed towards both the walls.

Figure 4 shows the case with a lower $W' = 0.38$. At $t = 0.47$ ms, the bubble has a nearly flat surface curvature on the top and bottom surface between the plates (side view). Subsequently, it acquires a concave surface curvature at $t = 0.73$ ms (side view) as the bubble starts collapsing. Between $t = 1.17$–1.40 ms at which time the bubble fully collapses, the bubble surface undergoes a few changes in curvature as seen in the side view. The curvature first changes from concave to convex between $t = 0.73$–1.17 ms and flattens at $t = 1.27$ ms. It becomes concave again by $t = 1.30$ ms, and then reverses to be convex by $t = 1.33$ ms. Finally the bubble collapses towards the center in a similar fashion as the bubble in Fig. 3.

The changes in curvature of the bubble surface seen in Figs. 2, 3, and 4 are plotted in Fig. 5(a). The plot shows the inverse of the surface curvature, i.e., $1/R_{\text{curve}}$ plotted against time. R_{curve} is obtained by measuring the radius of a circle, which matches the curved arc of the bubble at its central axis. For the convex curvature a circle matching the inside boundary of the bubble is used (i.e., a positive R_{curve}) while for the concave curvature, a circle matching the outside arc of the bubble is used (i.e., a negative R_{curve}). Figure 5(a) shows that the sign of the curvature changes once (convex to concave) for the bubble in Fig. 2, it changes twice for the case shown in Fig. 3 (i.e., convex to concave, and then back to convex), and it changes three times fully and comes close to a fourth change before collapse for the case shown in Fig. 4. The changes of curvature are indicated by solid circles (convex to concave) and dashed circles (concave to convex) in Fig. 5(a). A plot of the variation of the bubble radius with time is also given in Fig. 5(b).

About 100 experiments were conducted to measure the number of bubble oscillations that are observed before collapse as the gap width W' is varied. The observations are listed in Table I. Table I broadly delineates the ranges of W' and the nature of the bubble collapse, the number of bubble surface oscillations that are observed and the type of collapse (i.e.,

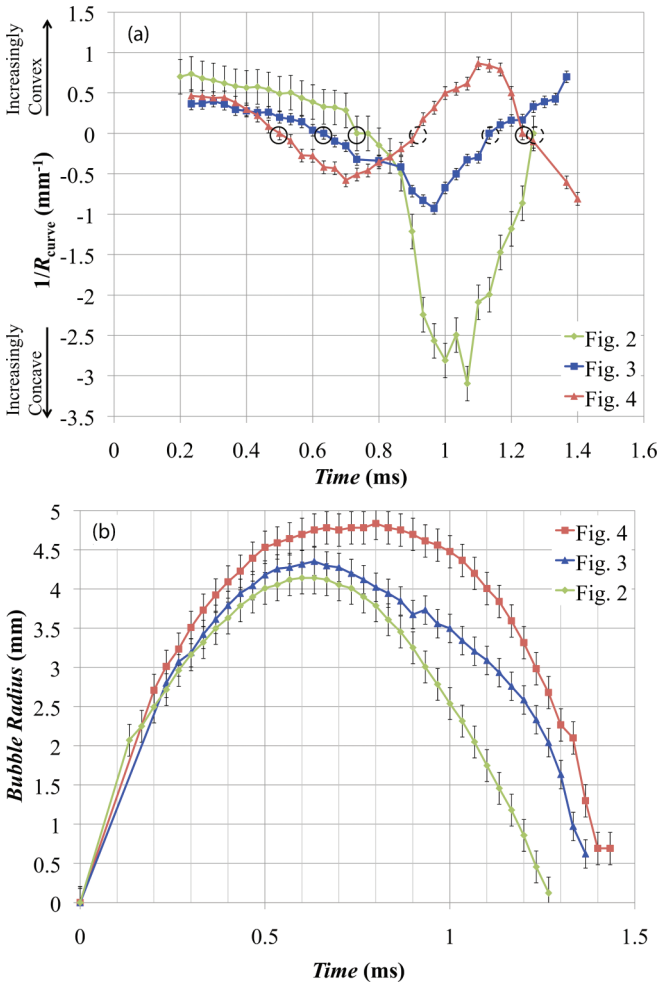

FIG. 5. (Color online) (a) The change in curvature of the bubble surface is quantified for the cases shown in Figs. 2, 3, and 4 using the inverse of the bubble radius of curvature $1/R_{\text{curve}}$ plotted against time (in milliseconds). Positive sign indicates a convex curvature while negative sign indicates a concave curvature. The circles indicate the points when the curvature changes. (b) The variation of the bubble radius measured vertically in the mid-plane between the two plates with respect to time is presented.

towards the center or split bubble collapse). Note that one oscillation here corresponds to going from convex surface to concave and back to convex.

In order to quantify the relative roles of inertia, viscosity, and surface tension, the Reynolds and Weber numbers were calculated. We consider just the case shown in Fig. 2 as an example. The gap width is $W = 3.7$ mm and the maximum bubble radius is $R_m = 4.3$ mm for this case. Based on the bubble expansion and collapse images, the typical bubble wall velocity during expansion is found to be $v = 6.5$ m/s. The values used are density $\rho = 1000$ kg/m^3, dynamic viscosity $\mu = 1$ mPas, and the surface tension for the air-water interface, $\sigma = 73 \times 10^{-3}$N/m. The gap width W is used as the characteristic length. The Reynolds number is thus calculated as

$$\text{Re} = \frac{v\rho W}{\mu} = 24\,050 \tag{1}$$

and the Weber number is given as

$$\text{We} = \frac{\rho v^2 W}{\sigma} = 2142. \tag{2}$$

The numbers indicate the predominant role of inertia in the bubble dynamics as compared to the effects of viscosity or surface tension. For any nonequilibrium bubble (not just within a narrow gap), its growth and collapse is governed by the inertia. When the bubble is created, due to the explosive nature of the bubble creation (such as by laser or spark discharge), the pressure inside the bubble is much larger than the surrounding, and so it overexpands and becomes much larger than the equilibrium radius. At the maximum bubble radius, the pressure inside the bubble is much lower than in the surrounding liquid. The bubble then starts collapsing. Thus, in the present case, while inertia seems to govern the overall expansion and collapse of the bubble, the surface oscillations of the bubble within the gap are not so easily explained. We also examined if the oscillations are due to capillary oscillations of the meniscus. A calculation of the characteristic time of the capillary vibrations is given as

$$\tau = \sqrt{\frac{\rho W^3}{\sigma}} = 26.3 \text{ ms}. \tag{3}$$

This is an order of magnitude higher than the time period of the bubble oscillations as noted from Figs. 2–4. As we shall show in the next section, the wettability of the plate surface also does not have any effect on the bubble dynamics. The physics behind this complex phenomenon of surface oscillations of the bubble in the gap evades a simple explanation and would require further research.

One possible qualitative explanation for the peculiar behavior of the bubble in Figs. 3 and 4 is now given. Lauterborn [14] points out that for an elongated collapsing bubble, more highly curved parts of the bubble surface, i.e., parts with low R_{curve} (say R_a) collapse faster than less curved parts, i.e., those with higher R_{curve}, (say R_b). He considered each of the parts equivalent to a spherical bubble of that radius (R_a, R_b) and since the collapse time (T_a, T_b respectively) is proportional to the bubble radius, the collapse time T_a will also be shorter than T_b, which means a faster collapse. Note that surface tension is not involved in this explanation.

TABLE I. The variation of the bubble surface oscillations close to the wall and collapse behavior with variation in W'.

Range of W'	Number of oscillations(N)	Collapse behaviour
$W' < 0.4$	$N > 1.5$	Collapse towards center
$0.4 < W' < 0.78$	$N = 1$	Collapse towards center
$0.78 > W' > 3.0$	$N = 0.5$	Bubble splits, collapses towards walls
$W' > 3.0$	–	Bubble collapses spherically or ellipsoidally

We now examine Figs. 3 and 4 in light of Lauterborn's explanation. In Fig. 3, at $t = 0.37$ ms, the bubble is more highly curved in its central portion (convex) as compared to the parts near the wall. Thus the central part of the bubble collapses first and leads to a flat surface. However, due to acquired inertia the central part continues collapsing to form a concave surface curvature. At $t = 0.93$ ms, the parts of the bubble attached to the two side walls (shown by two lines in Fig. 3) become more highly curved as compared to the center. Thus these portions collapse faster after $t = 0.93$ ms as compared to the central portion. The bubble surface flattens at $t = 1.13$ ms, and then due to inertia the sides continue to move faster, which leads again to a convex curvature. The bubble is also shrinking in size simultaneously and the inertia of the bubble due to shrinkage becomes more dominant around $t = 1.23$ ms and so the bubble collapses towards the center of the walls. Note here that the phenomenon is not in mechanical equilibrium at any time, and so there is no other force that is balancing inertia. By stating that inertia becomes dominant, we only mean that the inertia, which is always present, makes the bubble collapse before any further surface oscillations take place. If the bubble is sufficiently large as compared to the gap, i.e., has a lower $W' = W/R_m$, there could be a few more cycles of curvature changes before the inertia due to the collapsing bubble dominates the process. This is the case with Fig. 4 where we note one more cycle of such surface curvature changes. If the surface curvature when the bubble inertia becomes dominant is convex, the bubble will collapse towards the center as seen in the cases shown in Figs. 3 and 4. The effect of the cavity shape and inertia on the collapse dynamics is also shown for an asymmetric cavity in the work by Bergmann *et al.* [15].

B. Effect of surface wettability

We now present results on the effect of the surface wettability (i.e., the hydrophobic or hydrophilic nature of plate surface) on the bubble dynamics. For the hydrophobic plate experiments, two silanized glass plates were used. Figure 1(c) shows a water droplet on one of the silanized glass plates (hydrophobic) with a contact angle close to 90° as opposed to a contact angle of about 45° for an acrylic plate (hydrophilic).

Figure 6 shows a sequence of ten images of a bubble in the side view. There are two frames in each image. The left frame shows the observation for the side view of a symmetrically created bubble between the silanized glass plates. The right frame shows the corresponding observations for the bubble between the hydrophilic plates (same as the side-view images in Fig. 2). The other parameters related to the bubble (bubble size and gap width) were similar for the two cases. The hydrophobic experiment had a nondimensional gap width of $W' = 1.0$ ($W' = 0.86$ for the hydrophilic case) and a maximum bubble radius of $R_m = 3.7$ mm ($R_m = 4.3$ mm for hydrophilic case).

A comparison of the frames shows that the bubble between the hydrophobic plates exhibits very similar behavior to that between hydrophilic surfaces, under conditions of similar nondimensional gap widths W'. Experiments conducted on the hydrophobic plates with similar W' as that of Figs. 3 and 4 also supports this observation [13]. In Figure 6, the

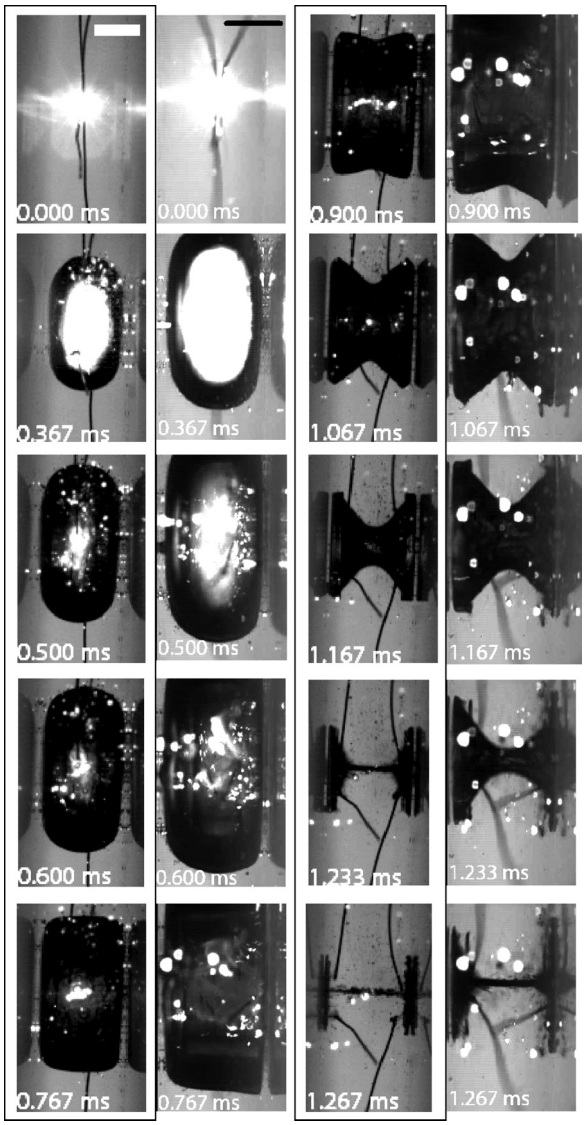

FIG. 6. A comparison of the side views of a bubble oscillating in the gap formed between two hydrophobic plates (left-side frame in each image) and two hydrophilic plates (right-side frame in each image) is shown. Note the similarity in the bubble behavior in terms of their expansion times, collapse, and jetting behavior. The images for the hydrophilic case are taken from Fig. 2. For the hydrophobic case, two silanized glass plates with a water-glass contact angle of 90° [Fig. 1(c)] are used. The bubble within this set of plates had a maximum radius of $R_m = 3.7$ mm, which is observed at $t = 0.600$ ms. The dimensional gap width $W = 3.7$ mm is the same as that for the hydrophilic case. The nondimensional gap width is $W' = 1.0$ for the hydrophobic case. The numbers at the bottom of each image indicates the time in ms. The scale bars are of length 2 mm.

bubble between the silanized glass plates reaches its maximum size at $t = 0.600$ ms with a convex surface as it expands. Subsequently the bubble surface starts flattening and then becomes concave as the bubble shrinks and then collapses with two jets towards each of the plates. The similarity between the bubble behaviors indicates that the surface characteristics do not have much of an effect on the bubble dynamics.

The reason for such bubble behavior is attributed to the presence of a thin film of liquid between the bubble and each

of the plates in both types of plates. Initially, the gap is filled with liquid and it is expected that as the bubble expands, it will push out the liquid in the gap where it is expanding. It appears though that even when the bubble expands against the plate, and even when a hydrophobic plate is used, there is always a thin film of liquid between the bubble and the plates that is not fully drained out. Further proof of this is found in the fact that the front-view movies often show an outward movement in Region R1 (best visible in the Supplemental movies [13]), which was explained by us as a thin film draining out radially. Unfortunately, it was not possible to measure the thickness of the film. The observations indicate that the bubble dynamics is dominated by this thin film and not so much by the surface properties.

IV. CONCLUSIONS

The dynamics of a bubble oscillating in a narrow gap is studied using two high-speed cameras to observe the behavior of the bubble from the side and the front simultaneously. The synchronized observations enable a better understanding of the mechanism behind the dark and light regions that have been reported in earlier studies involving visualization of oscillating bubbles in a narrow gap. A detailed explanation of the different regions is presented. Two different collapse behaviors of the bubble are described: (i) the bubble splitting in the center and collapsing with jets towards each of the plates, and (ii) the bubble collapsing towards the center between the plates. The collapse behavior is observed to depend on the surface oscillations that the bubble surface undergoes as the bubble collapses, which in turn depends on the nondimensional gap width $W' = W/R_m$ between the plates. A possible explanation of the surface oscillations and the collapse behavior of the bubble is given based on the observation that highly curved parts of a bubble collapse faster than those portions which are less curved. The behavior of the bubble is also unaffected by the surface wettability characteristics of the plate. The presence of a thin film of liquid between the bubble and each of the plates even as the bubble expands is proposed as the reason for such observation based on the images. The thin film of liquid adjacent to the bubble walls negates the effect of the surface characteristics on the bubble.

ACKNOWLEDGMENTS

The authors thank the Fluid Mechanics and Impact Mechanics Laboratories of the National University of Singapore (NUS) for their help with the fabrication of plates and allowing the usage of their high-speed cameras.

[1] R. Dijkink and C.-D. Ohl, Lab Chip **8**, 1676 (2008).
[2] S. Le Gac, E. Zwaan, A. van den Berg, and C. D. Ohl, Lab Chip **7**, 1666 (2007).
[3] G. N. Sankin, F. Yuan, and P. Zhong, Phys. Rev. Lett. **105**, 078101 (2010).
[4] P. Marmottant and S. Hilgenfeldt, Nature (London) **423**, 153 (2003).
[5] S. Z. Hua, F. Sachs, D. X. Yang, and H. D. Chopra, Anal. Chem. **74**, 6392 (2002).
[6] S. R. Gonzalez-Avila, F. Prabowo, A. Kumar, and C. D. Ohl, J. Memb. Sci. **415**, 776 (2012).
[7] V. V. Kucherenko and V. V. Shamko, J. Appl. Mech. and Tech. Phys **217**, 112 (1986).
[8] H. Ishida, C. Nuntadusit, H. Kimoto, T. Nakagawa, and T. Yamamoto, in CAV 2001: Fourth International Symposium on Cavitation, June 20-23, 2001, California Institute of Technology, Pasadena, CA, USA (unpublished).
[9] P. A. Quinto-Su, K. Y. Lim, and C.-D. Ohl, Phys. Rev. E **80**, 047301 (2009).
[10] S. R. Gonzalez-Avila, E. Klaseboer, B. C. Khoo, and C. D. Ohl, J. Fluid Mech. **682**, 241 (2011).
[11] K. S. F. Lew, E. Klaseboer, and B. C. Khoo, Sens. and Act. A **133**, 161 (2007).
[12] B. Karri, K. S. Pillai, E. Klaseboer, S. W. Ohl, and B. C. Khoo, Sens. and Act. A **169**, 151 (2011).
[13] See Supplemental Material at http://link.aps.org/supplemental/10.1103/PhysRevE.88.043006 for movie files.
[14] W. Lauterborn, Appl. Scient. Res. **38**, 165 (1982).
[15] R. Bergmann, D. van der Meer, S. Gekle, A. van der Bos, and D. Lohse, J. Fluid Mech. **633**, 381 (2009).